

RESEARCH ARTICLE

Sevoflurane protects rat brain endothelial barrier structure and function after hypoxia-reoxygenation injury

Tanja Restin^{1,2}*, Marie-Elisabeth Kajdi²*, Martin Schläpfer^{1,2}, Birgit Roth Z'graggen², Christa Booy², Claudia Dumrese³, Beatrice Beck-Schimmer^{1,2,4*}

1 Institute of Anesthesiology, University Hospital Zurich, Zurich, Switzerland, **2** Institute of Physiology, Zurich Centre for Integrative Human Physiology, University of Zurich, Zurich, Switzerland, **3** Flow Cytometry Facility, University of Zurich, Zurich, Switzerland, **4** Department of Anesthesiology, University of Illinois at Chicago, Chicago, United States of America

* These authors contributed equally to this work.

* beatrice.beckschimmer@uzh.ch



OPEN ACCESS

Citation: Restin T, Kajdi M-E, Schläpfer M, Roth Z'graggen B, Booy C, Dumrese C, et al. (2017) Sevoflurane protects rat brain endothelial barrier structure and function after hypoxia-reoxygenation injury. *PLoS ONE* 12(10): e0184973. <https://doi.org/10.1371/journal.pone.0184973>

Editor: Mária A. Deli, Hungarian Academy of Sciences, HUNGARY

Received: November 20, 2016

Accepted: September 5, 2017

Published: October 12, 2017

Copyright: © 2017 Restin et al. This is an open access article distributed under the terms of the [Creative Commons Attribution License](https://creativecommons.org/licenses/by/4.0/), which permits unrestricted use, distribution, and reproduction in any medium, provided the original author and source are credited.

Data Availability Statement: All relevant data are within the paper and its Supporting Information files.

Funding: This work was supported by a grant from the Zurich Centre of Integrative Human Physiology (ZIHP) of the University of Zurich, Zurich, Switzerland (BBS). TR's position is funded through the MD-PhD Program of the Swiss National Science Foundation (SNSF), Bern, Switzerland (323530_158128).

Abstract

Background

After cerebral injury blood-brain barrier disruption significantly impairs brain homeostasis. Volatile anesthetics have been shown to be protective in ischemia-reperfusion injury scenarios. Their impact on brain endothelial cells after hypoxia-reoxygenation (H/R) has not yet been studied in detail.

Methods

Rat brain endothelial cells (RBE4) were exposed to severe hypoxia and reoxygenated in air in the presence or absence of sevoflurane. Changes in dextran permeability and architecture of the cellular junctional proteins ZO-1 and β -catenin were measured. To determine necrosis and apoptosis rate DNA content, LDH release and caspase activity were quantified. The role of vascular endothelial growth factor (VEGF) as an inflammatory mediator increasing vascular permeability was assessed. At the same time, it was evaluated if sevoflurane effects are mediated through VEGF. Results were analyzed by unpaired t-tests or one way-analysis of variance followed by Bonferroni's correction.

Results

H/R led to a 172% increase in permeability ($p < 0.001$), cell swelling and qualitatively but not quantitatively modified expression of ZO-1, β -catenin and F-actin. In the presence of sevoflurane during reoxygenation, barrier function improved by 96% ($p = 0.042$) in parallel to a decrease of the cell size and less re-arranged junction proteins and F-actin. Sevoflurane-induced improvement of the barrier function could not be explained on the level of necrosis or apoptosis as they remained unchanged independent of the presence or absence of the volatile anesthetic. Increased expression of VEGF after H/R was attenuated by sevoflurane by 34% ($p = 0.004$). Barrier protection provided by sevoflurane was similar to the application

Competing interests: BBS has received a grant from Baxter AG as well as an honorarium from Maquet for a presentation, neither related to this work. All other authors declare that they do not have any conflicts of interest. This does not alter our adherence to PLOS ONE policies on sharing data and materials.

of a blocking VEGF-antibody. Furthermore, the protective effect of sevoflurane was abolished in the presence of recombinant VEGF.

Conclusions

In H/R-induced rat brain endothelial cell injury sevoflurane maintains endothelial barrier function through downregulation of VEGF, which is a key player not only in mediating injury, but also with regard to the protective effect of sevoflurane.

Introduction

The blood-brain barrier (BBB) strictly controls and regulates molecular exchange between the cerebral and vascular compartments, thereby safeguarding cerebral function [1]. Large protein complexes of endothelial cells, which form tight and adherens junctions, limit the paracellular flux [2]. The tight junction protein zonula occludens (ZO-1) and the adherens junction protein β -catenin are thereby key components contributing to normal barrier function [3]. Experimental models suggest that the generation of brain edema after BBB breakdown involves an early phase of leakage after 4 hours [4]. Particularly in brain injury, this early phase of brain edema formation involves an increase of vascular endothelial growth factor (VEGF) [5], one of the most potent permeability factors [6] [7]. VEGF directly modifies endothelial cell junctions [8, 9] [10] as well as the actin cytoskeleton [11] and may therefore promote further disruption of the blood-brain barrier, finally leading to neuronal malfunction [12].

Volatile anesthetics such as sevoflurane have been shown to sustain tissue integrity after ischemia-reperfusion (hypoxia-reoxygenation, H/R) injury in the heart [13], the liver [14], the lung [15] and the kidney [16]. They also affect the BBB and its function, with some authors postulating neuroprotective effects of volatile anesthetics [17, 18]. So far, limited information is available regarding the interaction of these anesthetics with the endothelial component of the BBB.

Working from the hypothesis that sevoflurane improves H/R-induced endothelial barrier dysfunction, we investigated whether the application of sevoflurane alters the permeability of rat brain endothelial cell (RBE4) layers and modifies important tight and adherens junctions. VEGF as one of the key permeability factors was determined in order to gain more insight into the possible signaling pathway.

Methods

Cell culture

RBE4 rat brain endothelial cells (P. Couraud, Cochin Institute, University Descartes, Paris) were grown on collagen-coated plates (rat tail collagen, 30–100 μ g (cm²)⁻¹ Sigma-Aldrich Chemie GmbH, Buchs, Switzerland) [19]. Media contained F10 and α -MEM in equal amounts, enriched with 10% fetal bovine serum (Life technologies, Zug, Switzerland), 2% 4-2-hydroxyethyl-1 piperazinethanesulfonic acid (Hepes) 1M (Sigma), 1ng/ml human basic fibroblast growth factor (PreproTech, London, UK) and 300 μ g ml⁻¹ geneticin (Sigma). Cells were incubated in humidified room air (humidity 70–90%) enriched with 5% CO₂.

Hypoxia and reoxygenation injury with or without sevoflurane

For all experiments, cells were seeded at a density of 50,000 cells ml⁻¹ and grown for 2–3 days to a confluency of 80–100%. Experiments started with either severe hypoxic (0.2% oxygen) or

normoxic (21% oxygen) treatment for 24 hours. For hypoxic exposure, cells were transferred to an anaerobic work station (Concept 400M, Ruskinn Technology, Baker Company, Sanford, Maine USA), while control cells remained in the normal incubator. Reoxygenation with sevoflurane was performed in Oxoid chambers (Oxoid, Hampshire, UK) for 4 hours in a mixture of room air enriched with 2.2% sevoflurane (Baxter Schweiz AG, Volketswil, Switzerland) and 5% CO₂, defined as postconditioning, in line with previous work carried out by our group [20].

Permeability assays

For permeability analysis, RBE4 cells were grown on collagen-coated TranswellTM chambers with 6.5mm-diameter polycarbonate inlays of pore size 0.4µm (Corning Incorporated, Corning, NY, USA). After exposure to H/R (or normoxia as control), medium was removed from the top compartment and fluorescein isothiocyanate (FITC)-dextran with a molecular weight of 40kD (Sigma) was added at a concentration of 1mg ml⁻¹. FITC-dextran permeation to the lower compartment was measured after 10, 20 and 30 minutes for the clearance curve analysis and after 30 minutes for determination of permeability. The amount of FITC permeation was quantified with the aid of a fluorometer (Infinite 200 pro, Tecan, Männedorf, Switzerland) at an excitation wave length of 490nm and an emission wave length of 525nm. The cleared volume was plotted against time and the permeability coefficient P_e was calculated according to Rist et al. [21]: $1/PS = 1/me - 1/mf$ and $P_e = PS/S$, where PS is defined as permeability surface area product, and S as surface area of the filter (0.331cm²). me and mf represent the slopes of the clearance curves of filters with (me) and filters without endothelial cells (mf) in ml = (cm³) min⁻¹.

Protein extraction

Cells were washed with ice-cold, phosphate-buffered saline (PBS, Kantonsapotheke Zurich, Switzerland; [S1 Table](#)) and homogenized in protein lysis buffer (containing 250mM Sucrose, 20mM Hepes, 10mM KCl, 1.5mM MgCl₂, 1mM EDTA, 1mM EGTA, 1mM DTT). 100µl of protease inhibitor mix (8340) and 50µl phosphatase inhibitor (P5726 and P0004), all purchased from Sigma, were added per 5x10⁶ cells. Protein concentrations were determined with the aid of a colorimetric assay based on the Bradford-dye binding method (Biorad Laboratories AG, Cressier, Switzerland), according to manufacturer's instructions.

Immunoblots

For ZO-1 and β-catenin quantification, proteins were denatured with sodium-dodecyl sulfate (SDS) and then loaded onto a polyacrylamide gel. After separation via electrophoresis, proteins were transferred to nitrocellulose membranes (material provided by Biorad and Sigma). Membranes were then blocked in 5% non-fat dry milk in tris-buffered saline (TBS; [S1 Table](#)). Primary antibodies were incubated at 4°C overnight with gentle shaking. Membranes were washed with TBS and 0.1% Tween 20 (Sigma) and consecutively incubated in the presence of the corresponding horseradish peroxidase (HRP)-conjugated secondary antibody. Band detection was performed with enhanced chemiluminescent substrate and visualized using luminescent image analyzer LAS-3000 (Fujifilm, Dielsdorf, Switzerland). Blot quantification was performed using ImageJ software (ImageJ, NIH, Maryland, USA). For protein detection with Western blotting, antibodies against ZO-1 were provided by Life technologies, for histone 3 by Cell Signaling (CST, Leiden, Netherlands), while secondary (HRP-coupled) antibodies were provided by Sigma and β-catenin antibodies by BD (Biosciences, Allschwil, Switzerland). The

protein amount was normalized to the mean protein expression in normoxia and adjusted for the histone 3 loading control.

Immunofluorescence

Cells were grown on poly-D-lysine hydrobromide ($50\text{--}100\mu\text{g (cm}^2\text{)}^{-1}$ Sigma) and collagen-coated glass cover slips (Karl Hecht GmbH&Co KG, Sondheim, Germany) and exposed to normoxia or severe hypoxia prior to 4h reoxygenation with or without sevoflurane as described. The monoclonal mouse anti- β -catenin antibody was used at a dilution of 1:500 (BD), monoclonal mouse anti-ZO-1 antibody at a dilution of 1:100 and phalloidin-Alexa 568 at 1:30 (both Life Technologies). The secondary anti-mouse Alexa-Fluor 488 antibody (Life technologies) was applied at a dilution of 1:500 and 4', 6-diamidino-2-phenylindole (DAPI, Roche Diagnostics, Mannheim, Germany) for nuclear staining was diluted to 1:1000.

Microscopy

Bright field pictures of RBE4 monolayers were taken with an inverted widefield fluorescence microscope (Leica DMI 6000, Leica Microsystems, Heerbrugg, Switzerland) and a cooled fluorescence monochrome camera (Leica DFC 350 FX, 1392 x 1040 pixel, pixel size 6.4 μm).

DNA quantification assay

In order to detect changes in DNA content, a quantification assay was performed using Bis-benzimide Hoechst 33342 (Sigma). Fluorescence was measured with a fluorometer (Tecan) at ex/em 360/460nm.

LDH release assay

For quantification of lactate dehydrogenase (LDH) release, the CytoTox[®] Non-Radioactive Cytotoxicity Assay (Promega, Dübendorf, Switzerland) was used. With the aid of this enzymatic assay, LDH, a cytosolic enzyme is measured in cell culture supernatants at an absorbance of 492nm with a spectrometer (Tecan). For maximum lysis control, lysis buffer was added 4 hours prior to detection.

Caspase assay

In order to quantify the cellular caspase activity, we used a selective caspase substrate for the caspases 3, 7 and 8 coupled to a fluorescent dye (Ac-Asp-Glu-Val-Asp-AMC; 3171v, Peptanova, Sandhausen, Germany). When the caspases are present, the fluorogenic AMC residue is cleaved and can be detected at ex/em 360/ 465nm with a fluorometer (Tecan).

Flow cytometry and cell size measurement

For flow and imaging cytometry cells were washed twice with 2.5mmol EDTA in PBS, detached with trypsin-EDTA solution (0.05%) (Thermo, Reinach, Switzerland) and put through a 35 μm cell strainer (Falcon, Corning, USA) after resuspension. The fixable viability dye eFluor[®] 660 (e Bioscience, Hatfield, UK) was used for viability analysis in accordance with the manufacturer's instructions. For cell analysis, BD FACS Canto II (BD) and Image Stream X Mark II (Merck, Millipore, Schaffhausen, Switzerland) were used. Doublets were excluded with the aid of a pulse geometry gate (FS-H x FS-A) in the flow cytometer and microscopically in the Image Stream analysis. Dead cells were excluded upon staining. For the flow cytometry analysis, the FSC-A voltage values of the first 500 cells in each experiment were analyzed and normalized to normoxia. For image stream analysis, cell size for every measured cell

was determined. ANOVA and Bonferroni correction was used for comparison of the different conditions.

VEGF analysis using enzyme linked immunoabsorbant assays

ELISA kits for VEGF were obtained from R&D Systems Europe (Abingdon, UK). Assays were performed according to the manufacturer's instructions. Cells were grown on collagen-coated plates at a density of $50,000 \text{ ml}^{-1}$ for 2 days and exposed to severe hypoxia (24 hours) and reoxygenation (4 hours) with or without sevoflurane as described above. Afterwards, cell supernatants were collected and VEGF protein content quantified.

Addition of VEGF antibody and recombinant VEGF during the reoxygenation period

In order to assess the effect of VEGF during the reoxygenation period, permeability experiments were performed as described above. During the 4-hour reoxygenation period, VEGF antibody (AF564 goat anti-rat VEGF antibody, R&D, Abingdon, UK) was added at a concentration of $1 \mu\text{g/ml}$, the corresponding goat IgG served as a control as previously described [22]. In order to assess whether the effect of sevoflurane can be reversed by recombinant VEGF (rVEGF), VEGF protein was added at a concentration of 50 ng/ml [23].

Data analysis, statistics and graphs

Data are graphed with mean values with standard deviation represented as whiskers. Each assay was performed at least three times independently. Statistical analysis was performed using either paired, two tailed-t-tests for two groups or one way-analysis of variance (ANOVA) for more than two groups, with Bonferroni's correction for multiple comparisons. Flow cytometry data was analyzed using FACS DIVA 8.0.1 and FlowJo software. Image stream data were processed using Image Data Exploration and Analysis software (IDEAS) (Amnis, Seattle, WA, USA). Densitometry analysis and areas of phalloidin staining were assessed with the aid of image J. To identify actin tangles, a threshold of 37 was set and pixels above 37 were defined as actin positive. Below this cut-off, actin was not clearly positive. The number of actin positive pixels per image was then counted on binary images (representing total phalloidin of the entire cells). For subcellular analysis, the program "CellProfiler" (www.cellprofiler.org) [24] was used to identify the nuclei (pixel range between 35–120 pixel units) in each image as primary objects. In a next step, the cell cytoplasm was identified as secondary object characterized by the area surrounding the nucleus limited by continuous F-actin tangles at the cell border. Identification of the secondary objects was performed with the aid of the watershed tool. Then, the integrated F-actin staining intensity was evaluated for each cell. Data was analyzed and graphs created using Graph Pad Prism 6 (San Diego, CA, USA) and IBM® SPSS statistics 22.0.0.0.

Results

The complete data set for the manuscript can be found in supplementary online content [S2 Table](#). All relevant data are within the paper and its Supporting Information files.

Sevoflurane postconditioning improves barrier function in rat brain endothelial cells exposed to H/R

When plotting the FITC-clearance against time, the curves showed a linear relationship. H/R injury induced an increase in cleared volume over time, while sevoflurane postconditioning reduced it ([Fig 1A](#)). The corresponding P_e values in normoxia were $6 \pm 1.5 \times 10^{-3} \text{ cm/min}$. After

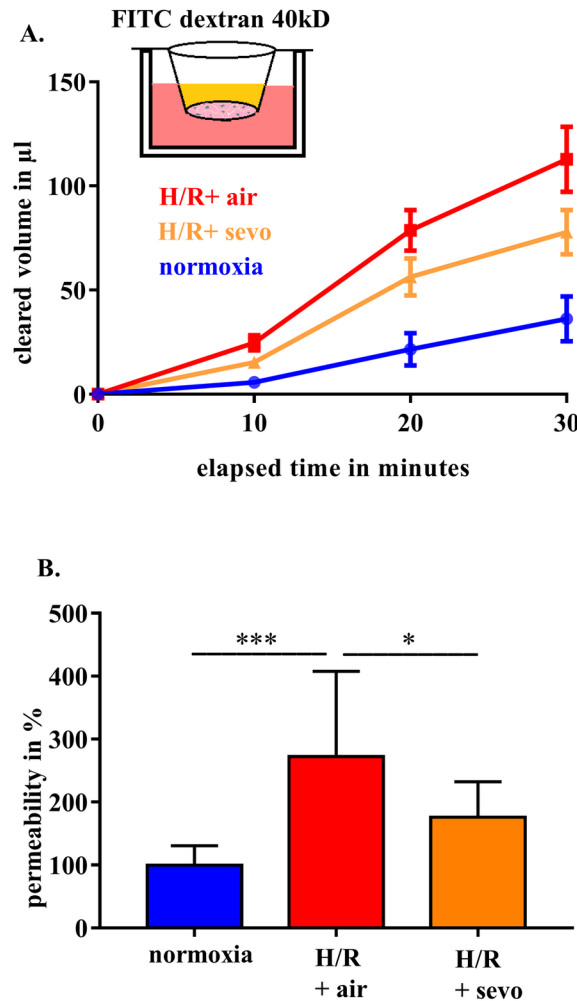


Fig 1. Sevoflurane and barrier function in rat brain endothelial cells in H/R injury. RBE4 cells were exposed to severe hypoxia (0.2% oxygen) for 24 hours, followed by a 4-hour period of reoxygenation in air (H/R+air) or air enriched with sevoflurane (H/R+sevo). Cells in the normoxia group remained in a normal cell culture environment with 21% oxygen for the full 28 hours. Clearance and permeability were determined using FITC-dextran. FITC clearance was measured after 10, 20 and 30 minutes (A). Permeability was assessed after 30 minutes and normoxia was defined as 100% (B). Bar graphs show mean values and standard deviations. n = 11 in each group, analyzed with ANOVA and Bonferroni correction. *** p<0.001, * p<0.05.

<https://doi.org/10.1371/journal.pone.0184973.g001>

30 minutes, a 172% increase of permeability of the RBE4 monolayer was observed (normoxia: 100±31%, H/R+air: 272±135%, p<0.001). With the addition of sevoflurane during the reoxygenation period, barrier function significantly improved, leading to a 96% decrease in permeability (p<0.05; Fig 1B).

Sevoflurane postconditioning preserves cellular arrangement of junction proteins in rat brain endothelial cells in H/R injury

Alteration of tight and adherens junction components, namely ZO-1 and β-catenin in RBE4 cells, were assessed in response to H/R+air as illustrated in Fig 2A and Fig 2B. Under H/R+air tight and adherens junction proteins in the larger cells appear disrupted with better maintained morphology in the presence of sevoflurane. For further quantification, Western blot analysis was performed and showed no alteration in the total amount of ZO-1 or β-catenin

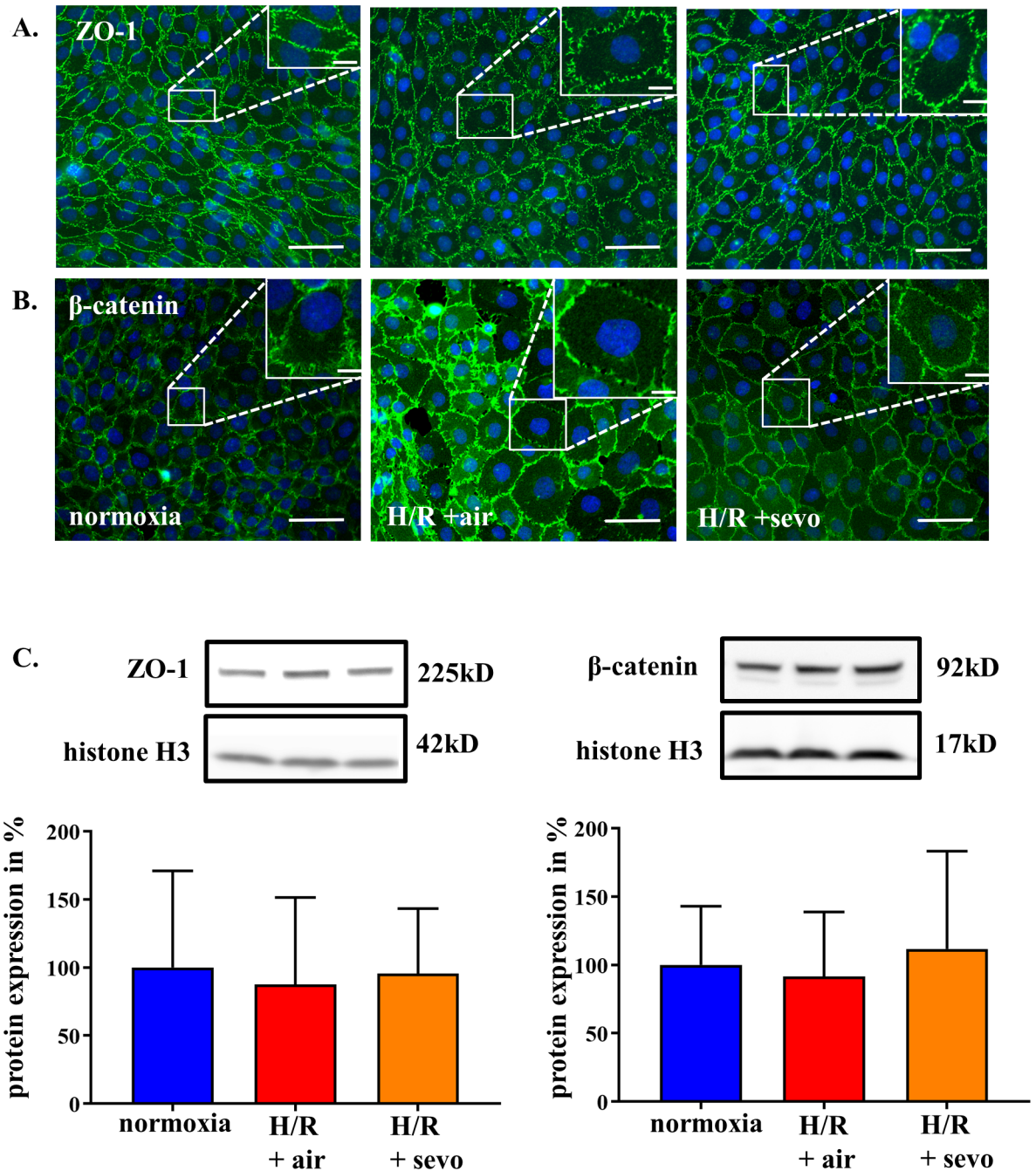


Fig 2. Sevoflurane and architecture of intercellular junction proteins of rat brain endothelial cells in H/R injury. RBE4 cells were exposed to severe hypoxia (0.2% oxygen) for 24 hours, followed by a 4-hour period of reoxygenation in air (H/R+air) or air enriched with sevoflurane (H/R+sevo). Cells in the normoxia group remained in a normal cell culture environment with 21% oxygen for the full 28 hours. After fixation, the junctional molecules ZO-1 (A) and β -catenin (B) were stained using according antibodies as shown in green, and the nucleus was visualized with DAPI as demonstrated in blue. Western blots were performed with according antibodies against ZO-1 and β -catenin with histone 3 as control (C). Bar graphs show mean values and standard deviations. n = 4 separate stainings for each group and antibody, ZO-1 and β -catenin protein analysis n = 6 per group, analyzed with ANOVA and Bonferroni correction.

<https://doi.org/10.1371/journal.pone.0184973.g002>

(Fig 2C). However, cell size increased under H/R+air, while sevoflurane partially mitigated this swelling (Fig 2A).

Sevoflurane does not improve H/R-induced decrease of DNA content, increase of LDH and enhanced caspase activity

In a further step, it was determined whether changes in permeability and tight junction organization were associated with a reduced cell number and/or an increased necrosis or apoptosis rate. Compared to cells incubated under normoxic conditions, H/R decreased the DNA content by 20% (normoxia $100 \pm 3\%$ H/R+air $81 \pm 2\%$, $p < 0.001$) (Fig 3A), increased LDH release by 4% (normoxia $21 \pm 4\%$, H/R+air $25 \pm 4\%$, $p < 0.01$) (Fig 3B) and increased caspase activity by 71% (normoxia $100 \pm 21\%$, H/R+air $171 \pm 67\%$, $p < 0.001$) (Fig 3C). However, addition of 2.2% sevoflurane during the reoxygenation period did not have an impact on these three parameters (Fig 3).

Sevoflurane postconditioning preserves cell size in H/R injury

To verify observed changes of cell size in Fig 2 further experiments were performed using flow cytometry and image stream. H/R induced a mean forward scatter area (FSC-A) increase by 8.6% ($p < 0.001$), while sevoflurane treatment decreased this change to 3.5% ($p < 0.001$) (Fig 4A). This FSC-A-change correlated well with cell size changes in image stream analysis, which revealed a mean area of $237 \mu\text{m}^2$ for cells grown in normoxia, a cell size increase after H/R, which was more pronounced when cells were reoxygenated with air (average area $250 \mu\text{m}^2$) compared to reoxygenation with sevoflurane (average area $242 \mu\text{m}^2$). These changes were significant for each experiment ($p < 0.001$ for normoxia vs. H/R + air and $p < 0.001$ for H/R + air vs. H/R + sevo) (Fig 4B).

Sevoflurane acts on F-actin cytoskeleton

In order to know whether the volume changes translate into changes of the cytoskeleton phalloidin stainings were performed. RBE4 cells grown in normoxia showed predominantly membrane associated F-actin, while after H/R the normal F-actin structure was disrupted. In the presence of sevoflurane during reoxygenation F-actin was associated in bundles and redirected to the cell membrane (Fig 5A and Fig 5B). While this qualitative difference was observed, total F-actin did not differ (Fig 5C). Segmentation of each cell into cytoplasm and nucleus revealed an increase of F-actin in response to H/R+air both in the cytoplasm and in the nuclei compared to H/R+sevo (Fig 5D and Fig 5E), with F-actin primarily localized at the cell membrane. Detailed evaluation revealed that the amount of F-actin within the cell cytoplasm increased by 55% ($p < 0.001$) when exposed to H/R+air. Reoxygenation in the presence of sevoflurane (H/R+sevo) attenuated this by 22% compared to H/R+air ($p < 0.005$) (Fig 5D). Additionally, after H/R+air, more F-actin tangles were observed in the nucleus area compared to the normoxic condition (22% increase, $p < 0.001$). The reduction of integrated intensity in the nuclear area after sevoflurane postconditioning was 48% ($p < 0.001$) (Fig 5E).

Sevoflurane postconditioning attenuates increased VEGF levels after H/R injury

VEGF protein concentration was measured in the RBE4 cell supernatant. This mediator VEGF was hardly detectable in normoxia at $167 \pm 82 \text{pg ml}^{-1}$ (Fig 6A). However, the concentration significantly increased in response to H/R+air to 2597pg ml^{-1} ($\pm 888 \text{pg ml}^{-1}$, $p < 0.001$), while sevoflurane exposure reduced VEGF levels by 878pg ml^{-1} ($p < 0.01$). In order to know whether the changes in permeability might be mediated by VEGF, this inflammatory mediator was blocked and the increase in permeability was mitigated (H/R+air $237 \pm 90\%$ vs. H/R+VEGF antibody $118 \pm 42\%$ ($p = 0.001$) compared to the normoxic control (Fig 6B). Addition

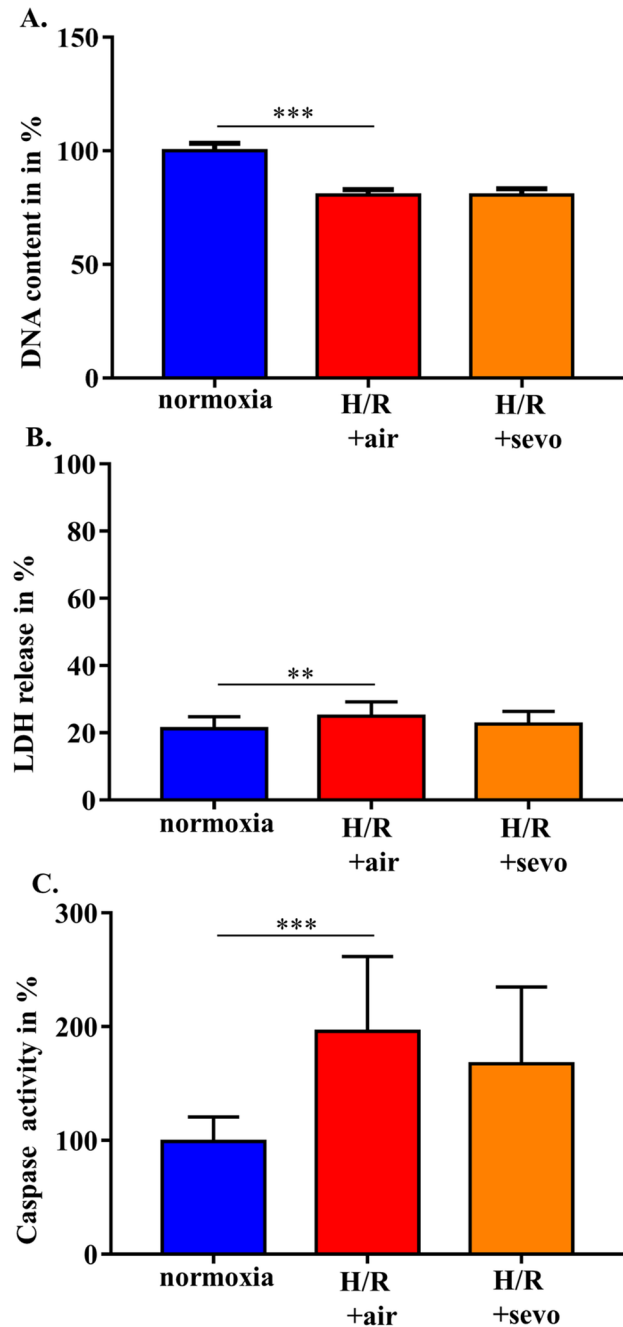


Fig 3. Sevoflurane and DNA content, LDH release and caspase activity in rat brain endothelial cells in H/R injury. RBE4 cells were exposed to severe hypoxia (0.2% oxygen) for 24 hours, followed by a 4-hour period of reoxygenation in air (H/R+air) or air enriched with sevoflurane (H/R+sevo). Cells in the normoxia group remained in a normal cell culture environment with 21% oxygen for the full 28 hours. Determination of DNA was performed using fluorogenic bisbenzimidazole (A). LDH release was measured with the aid of a non-radioactive cytotoxicity assay (B). Caspase 3/7/8 activity was assessed with a cleavage assay (C). Bar graphs show mean values and standard deviations. n = 18 for each group (DNA content), n = 24 for each group (LDH release and caspase activity), analyzed with ANOVA and Bonferroni correction. ** p<0.01, *** p<0.001.

<https://doi.org/10.1371/journal.pone.0184973.g003>

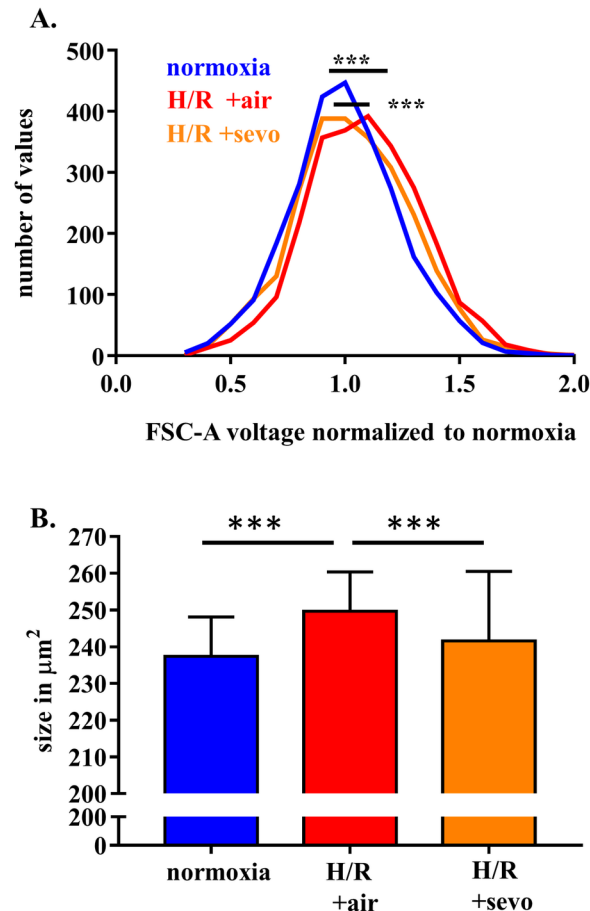


Fig 4. Sevoflurane and rat brain endothelial cell size in H/R injury. RBE4 cells were exposed to severe hypoxia (0.2% oxygen) for 24 hours, followed by a 4-hour period of reoxygenation in air (H/R+air) or air enriched with sevoflurane (H/R+sevo). Cells in the normoxia group remained in a normal cell culture environment with 21% oxygen for the full 28 hours. After detachment with trypsin-EDTA and viability staining, cells were analyzed with the flow cytometer or image stream, respectively. FSC-A as an indirect measure of cell size was assessed in conventional flow cytometry (A), while the cell size of each cell was assessed with the image stream method (B). The histogram shows the distribution pattern of FSC-A seen in the flow cytometry. $n = 5$ independent experiments, with 500 cells analyzed in each condition. The bar graph shows mean values and standard deviations. $n = 4$ Image stream X experiments, at least 20,000 cells analyzed in each condition. Analysis with one way ANOVA and Bonferroni correction. *** $p < 0.001$.

<https://doi.org/10.1371/journal.pone.0184973.g004>

of rVEGF during reoxygenation abolished the sevoflurane-mediated beneficial effect on permeability (Fig 6C).

Discussion

Blood-brain barrier disruption is highly relevant in the pathogenesis of secondary brain damage after brain injury [12, 25]. In the present study, we show for the first time that sevoflurane treatment during the early reoxygenation period following severe hypoxia promotes the maintenance of BBB structure and function in rat brain endothelial cells. The permeability patterns of the RBE4 grown on Transwells™ were comparable with the data shown by Rist et al. [21] with P_e -values of 6×10^{-3} cm per minute in normoxia.

The increased permeability for macromolecular FITC dextran after H/R reflects a severe barrier disruption in RBE4 monolayers, consistent with previously published data [26]. These

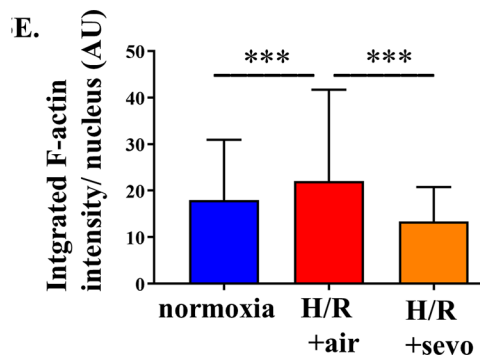
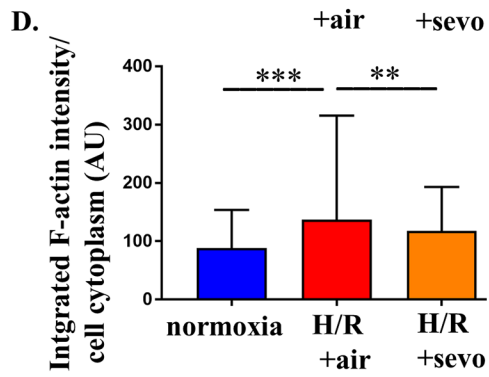
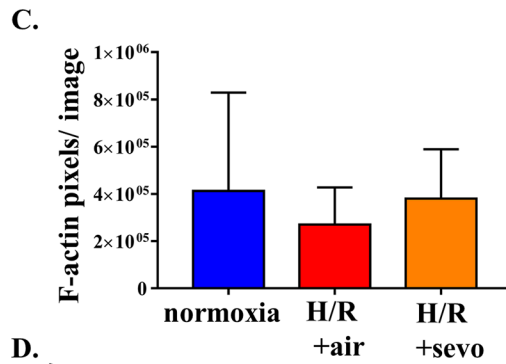
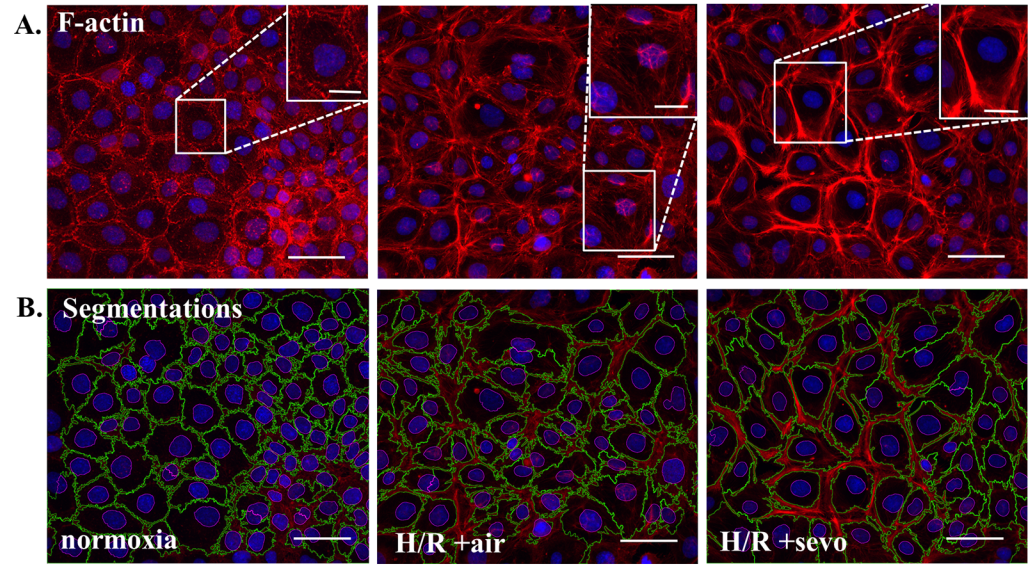


Fig 5. Sevoflurane and rat brain endothelial cell organization of actin cytoskeleton after H/R injury.

RBE4 cells were exposed to severe hypoxia (0.2% oxygen) for 24 hours, followed by a 4-hour period of reoxygenation in air (H/R+air) or air enriched with sevoflurane (H/R+sevo). Cells in the normoxia group remained in a normal cell culture environment with 21% oxygen for the full 28 hours. Phalloidin staining visualizes F-actin tangles as seen in red, blue DAPI staining shows cell nuclei (A). Quantitative assessment of F-actin was performed by determination of F-actin pixels per image above the threshold of 37 in Image J (A, C). To further evaluate morphological changes, segmentation was performed targeting the cytoplasm surrounded with green lines and the nucleus surrounded with a cyan line (B). The integrated intensity in these regions of interest was then analyzed (cytoplasm, D) and (nucleus, E). $n = 3$ independent experiments with 3 analyzed images per condition per experiment. Analysis of the mean of each experiment with one way ANOVA and Bonferroni correction.

<https://doi.org/10.1371/journal.pone.0184973.g005>

changes can be explained by dysregulated tight and adherens junction proteins [27], which normally limit the paracellular flux [28] and orchestrate intercellular contact formation [29]. ZO-1-depleted cells lack functional junctions [29], and endothelial cells with conditional inactivation of β -catenin exhibit reduced cell adhesion and increased permeability [30]. Interestingly, in our experiments, the amount of tight and adherens junction proteins tested was not reduced after H/R, suggesting that application of sevoflurane helps to reorganize the existing protein structures without any quantitative change. Although beyond the scope of our experiments, it is tempting to further assess if severe hypoxia alone modifies junctional integrity and to which extend the reoxygenation process changes these dynamics.

We showed that H/R injury in brain endothelial cells induces both necrosis as reflected by decreased DNA content and increased LDH release as well as apoptosis, which was defined by increased caspase activity. One would expect an improved barrier function in the presence of sevoflurane lowering death rate. However, the application of sevoflurane did not impact on necrosis or on apoptosis. Sevoflurane rather influenced cell size and structural organization of the endothelial cells and thereby counteracted impaired barrier function.

Swelling of the endothelial cells due to edema formation is described as a prominent feature after H/R [31], and may indeed lead to disruption of the junctions. It is quantified by both flow cytometry and image stream. While the voltage of the forward scatter in flow cytometry analysis can both be modified by cell size and the refractive index differences of fluids and cells [32], microscopical analysis via image stream can accurately determine the cell size [33]. When comparing the images of cells either reoxygenated with air or with sevoflurane, computational analysis identified the cell size as differentiating factor between the treatment groups.

One of the most potent vascular permeability factors is VEGF [6]. In our experimental setting, this signaling molecule was significantly upregulated in response to H/R. At the same time, sevoflurane reduced VEGF expression relative to H/R without sevoflurane postconditioning. VEGF increases nuclear levels of β -catenin and modifies its subcellular distribution without changing the total cell amount of this adherens junction protein [34]. Besides this direct action on tight and adherens junction proteins [34, 35]. VEGF may also have an indirect effect on cell size [36]. *In vivo* it has been shown that an early blockade of VEGF reduces brain tissue edema formation in mice after stroke [37] and that it also attenuates on a cellular level the extent of cell swelling induced by cytotoxic edema after cerebral venous infarction in rats [38]. In our experiments, we could demonstrate on a cellular level, that H/R induces cell swelling, which is mitigated by sevoflurane treatment, possibly via downregulation of VEGF.

It is important to realize that F-actin structure and regulation [39], which is supposed to be involved in the spatial control and stabilization of cellular junctions [40], may be another component being influenced in the presence of sevoflurane. H/R injury caused disruption of F-actin, sevoflurane, however, stabilized arrangement of F-actin.

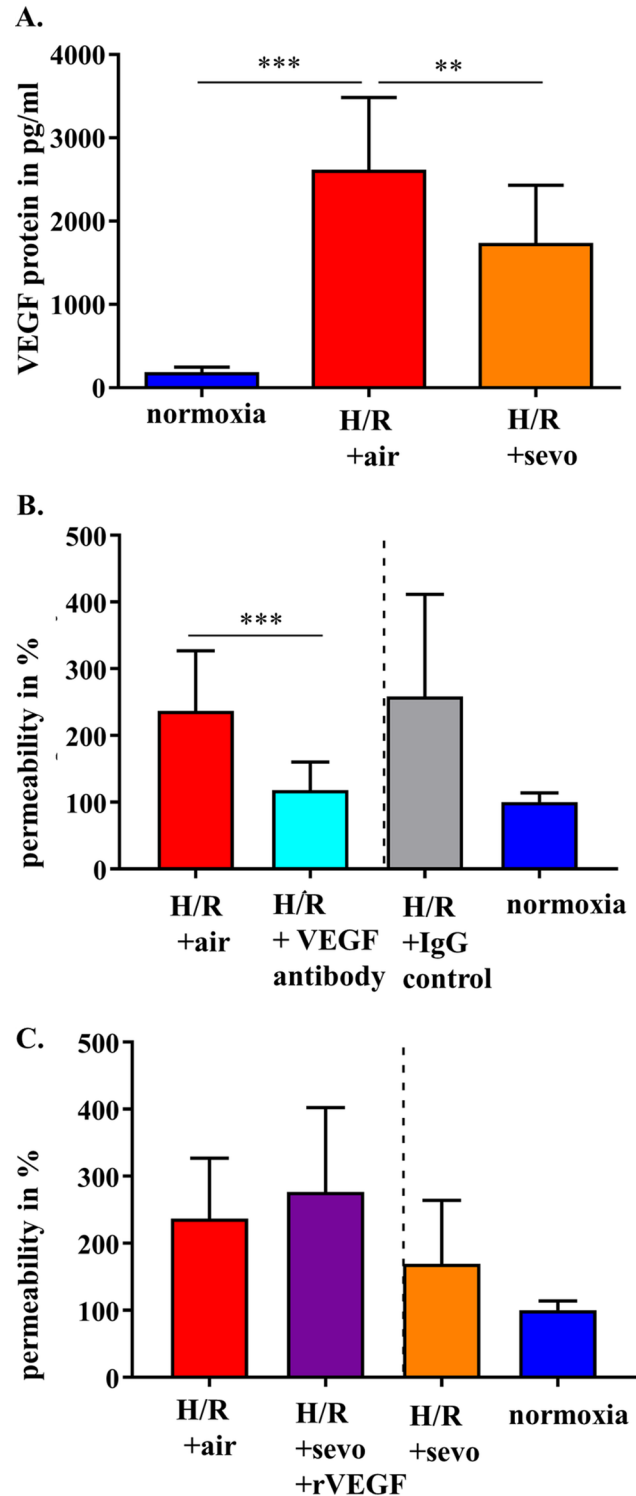


Fig 6. Sevoflurane and the role of VEGF expressed by rat brain endothelial cell in H/R. RBE4 cells were exposed to severe hypoxia (0.2% oxygen) for 24 hours, followed by a 4-hour reoxygenation period in air (H/R +air) or air enriched with sevoflurane (H/R+sevo). Cells in the normoxia group remained in a normal cell culture environment with 21% oxygen for the full 28 hours. VEGF protein was determined in the supernatant using ELISA (A). RBE4 cells were exposed to hypoxia (0.2% oxygen) for 24 hours, followed by a 4-hour reoxygenation period in air (H/R+air) or air enriched with a VEGF antibody (1 µg/ml). As a control iso IgG was used. Permeability was assessed at 30 minutes using FITC-dextran. Normoxia was defined as 100% (B). RBE4 cells were exposed

to hypoxia (0.2% oxygen) for 24 hours, followed by a 4-hour reoxygenation period in air (H/R+air) and air enriched with sevoflurane (H/R+sevo) in the presence of rVEGF (50ng/ml). Permeability was assessed at 30 minutes using FITC-dextran. Normoxia was defined as 100% (C). Bar graphs show mean values and standard deviations. n = 11 in normoxia and n = 15 in H/R+air and H/R+sevo (A) n = 20 in H/R+air and n = 12 in VEGF and VEGF IgG (B) n = 17 in H/R + air and n = 6 in H/R+sevo+rVEGF Analysis with one way ANOVA and Bonferroni correction. *** p<0.001 ** p<0.01.

<https://doi.org/10.1371/journal.pone.0184973.g006>

While an established and elegant model [19], our *in vitro* approach has its limitations. The effects detected are specific for endothelial cells and cannot reflect the full complexity of the cellular interplay at the BBB including astrocytes and pericytes. Moreover, every immortalized cell line is modified to allow cell processing and tissue specific functions may not be fully represented [41]. Finally, although we detected that sevoflurane reduces VEGF protein secretion, which is potentially involved in junctional and cellular changes, we did not elucidate the detailed signaling pathway.

In summary, we show that the impairment of barrier function in brain endothelial cells is improved by sevoflurane postconditioning. This anesthetic acts on tight and adherens junctions, possibly through the attenuation of injury-induced production of VEGF. This signaling pathway may be an interesting future drug target, but needs to be further assessed in detail in *in vivo* studies.

Supporting information

S1 Table. Composition of phosphate-buffered saline as tris-buffered saline.

(DOCX)

S2 Table. Relevant data of the study. All data have been summarized in this table.

(XLSX)

Acknowledgments

We thank Emanuela Keller, MD., Neurointensive Care Unit, Department of Neurosurgery, University Hospital Zurich, Zurich, Switzerland for scientific input, grant acquisition for the project and critical proofreading of the manuscript.

We thank Pierre-Olivier Couraud, PhD, Institut Cochin, Paris, France for kindly providing us with RBE4 cells.

We thank Jana Döhner, PhD and Caroline Aemisegger, Center of Microscopy and Image Analysis, University of Zurich, Zurich, Switzerland for technical support during microscopic image acquisition and analysis. Moritz Kirschmann, Center of Microscopy and Image Analysis, was a big help to perform cell segmentation and the actin analysis with Cell profiler. We thank Urs Ziegler, head of the Center of Microscopy and Image Analysis, for his precious advice in image acquisition and analysis.

We are grateful to Christopher Tsatsaris, MD, Institute for Physiology, University of Zurich, Zurich, Switzerland for technical support during protein quantification and we thank Martin Urner, MD. Institute for Physiology, University of Zurich, Zurich, Switzerland for statistical advice and proofreading of the manuscript. We thank Tim Kileen, MD, St. Gallen, Switzerland for proofreading of the manuscript.

Author Contributions

Conceptualization: Marie-Elisabeth Kajdi, Martin Schläpfer, Claudia Dumrese, Beatrice Beck-Schimmer.

Data curation: Martin Schläpfer, Beatrice Beck-Schimmer.

Formal analysis: Tanja Restin, Martin Schläpfer, Birgit Roth Z'graggen, Christa Booy.

Funding acquisition: Beatrice Beck-Schimmer.

Investigation: Marie-Elisabeth Kajdi, Martin Schläpfer, Birgit Roth Z'graggen, Christa Booy, Beatrice Beck-Schimmer.

Methodology: Tanja Restin, Marie-Elisabeth Kajdi, Martin Schläpfer, Birgit Roth Z'graggen, Christa Booy, Claudia Dumrese, Beatrice Beck-Schimmer.

Project administration: Beatrice Beck-Schimmer.

Resources: Beatrice Beck-Schimmer.

Software: Tanja Restin, Claudia Dumrese.

Supervision: Birgit Roth Z'graggen, Beatrice Beck-Schimmer.

Validation: Martin Schläpfer, Birgit Roth Z'graggen, Beatrice Beck-Schimmer.

Writing – original draft: Tanja Restin, Martin Schläpfer, Birgit Roth Z'graggen, Claudia Dumrese, Beatrice Beck-Schimmer.

Writing – review & editing: Marie-Elisabeth Kajdi, Martin Schläpfer, Birgit Roth Z'graggen, Christa Booy, Claudia Dumrese, Beatrice Beck-Schimmer.

References

1. Daneman R. The blood-brain barrier in health and disease. *Ann Neurol.* 2012; 72(5):648–72. <https://doi.org/10.1002/ana.23648> PMID: 23280789.
2. Abbott NJ, Friedman A. Overview and introduction: the blood-brain barrier in health and disease. *Epilepsia.* 2012; 53 Suppl 6:1–6. <https://doi.org/10.1111/j.1528-1167.2012.03696.x> PMID: 23134489; PubMed Central PMCID: PMC3625728.
3. Tietz S, Engelhardt B. Brain barriers: Crosstalk between complex tight junctions and adherens junctions. *J Cell Biol.* 2015; 209(4):493–506. <https://doi.org/10.1083/jcb.201412147> PMID: 26008742; PubMed Central PMCID: PMC4442813.
4. Pillai DR, Dittmar MS, Baldaranov D, Heidemann RM, Henning EC, Schuierer G, et al. Cerebral ischemia-reperfusion injury in rats—a 3 T MRI study on biphasic blood-brain barrier opening and the dynamics of edema formation. *J Cereb Blood Flow Metab.* 2009; 29(11):1846–55. <https://doi.org/10.1038/jcbfm.2009.106> PMID: 19654585; PubMed Central PMCID: PMC4442813.
5. Chodobski A, Chung I, Kozniowska E, Ivanenko T, Chang W, Harrington JF, et al. Early neutrophilic expression of vascular endothelial growth factor after traumatic brain injury. *Neuroscience.* 2003; 122(4):853–67. PMID: 14643756.
6. Senger DR, Van de Water L, Brown LF, Nagy JA, Yeo KT, Yeo TK, et al. Vascular permeability factor (VPF, VEGF) in tumor biology. *Cancer Metastasis Rev.* 1993; 12(3–4):303–24. PMID: 8281615.
7. Olsson AK, Dimberg A, Kreuger J, Claesson-Welsh L. VEGF receptor signalling—in control of vascular function. *Nat Rev Mol Cell Biol.* 2006; 7(5):359–71. <https://doi.org/10.1038/nrm1911> PMID: 16633338.
8. Hippenstiel S, Krull M, Ikemann A, Risau W, Clauss M, Suttrop N. VEGF induces hyperpermeability by a direct action on endothelial cells. *Am J Physiol.* 1998; 274(5 Pt 1):L678–84. PMID: 9612282.
9. Fischer S, Wobben M, Marti HH, Renz D, Schaper W. Hypoxia-induced hyperpermeability in brain microvessel endothelial cells involves VEGF-mediated changes in the expression of zonula occludens-1. *Microvasc Res.* 2002; 63(1):70–80. <https://doi.org/10.1006/mvre.2001.2367> PMID: 11749074.
10. Gavard J, Gutkind JS. VEGF controls endothelial-cell permeability by promoting the beta-arrestin-dependent endocytosis of VE-cadherin. *Nat Cell Biol.* 2006; 8(11):1223–34. <https://doi.org/10.1038/ncb1486> PMID: 17060906.
11. Bae MJ, Lee YM, Kim YH, Han HS, Lee HJ. Utilizing Ultrasound to Transiently Increase Blood-Brain Barrier Permeability, Modulate of the Tight Junction Proteins, and Alter Cytoskeletal Structure. *Curr Neurovasc Res.* 2015; 12(4):375–83. PMID: 26238467.

12. Obermeier B, Daneman R, Ransohoff RM. Development, maintenance and disruption of the blood-brain barrier. *Nat Med.* 2013; 19(12):1584–96. <https://doi.org/10.1038/nm.3407> PMID: 24309662
13. De Hert SG, Van der Linden PJ, Cromheecke S, Meeus R, Nelis A, Van Reeth V, et al. Cardioprotective properties of sevoflurane in patients undergoing coronary surgery with cardiopulmonary bypass are related to the modalities of its administration. *Anesthesiology.* 2004; 101(2):299–310. PMID: 15277911.
14. Beck-Schimmer B, Breitenstein S, Urech S, De Conno E, Wittlinger M, Puhon M, et al. A randomized controlled trial on pharmacological preconditioning in liver surgery using a volatile anesthetic. *Ann Surg.* 2008; 248(6):909–18. <https://doi.org/10.1097/SLA.0b013e31818f3dda> PMID: 19092335.
15. Voigtsberger S, Lachmann RA, Leutert AC, Schlapfer M, Booy C, Reyes L, et al. Sevoflurane ameliorates gas exchange and attenuates lung damage in experimental lipopolysaccharide-induced lung injury. *Anesthesiology.* 2009; 111(6):1238–48. <https://doi.org/10.1097/ALN.0b013e3181bdf857> PMID: 19934867.
16. Lee HT, Ota-Setlik A, Fu Y, Nasr SH, Emala CW. Differential protective effects of volatile anesthetics against renal ischemia-reperfusion injury in vivo. *Anesthesiology.* 2004; 101(6):1313–24. PMID: 15564938.
17. Adamczyk S, Robin E, Simerabet M, Kipnis E, Tavernier B, Vallet B, et al. Sevoflurane pre- and post-conditioning protect the brain via the mitochondrial K ATP channel. *Br J Anaesth.* 2010; 104(2):191–200. <https://doi.org/10.1093/bja/aep365> PMID: 20086064.
18. Thal SC, Luh C, Schaible EV, Timaru-Kast R, Hedrich J, Luhmann HJ, et al. Volatile anesthetics influence blood-brain barrier integrity by modulation of tight junction protein expression in traumatic brain injury. *PLoS One.* 2012; 7(12):e50752. <https://doi.org/10.1371/journal.pone.0050752> PMID: 23251381; PubMed Central PMCID: PMC3519465.
19. Roux F, Couraud PO. Rat brain endothelial cell lines for the study of blood-brain barrier permeability and transport functions. *Cell Mol Neurobiol.* 2005; 25(1):41–58. PMID: 15962508.
20. Yue T, Roth Z'graggen B, Blumenthal S, Neff SB, Reyes L, Booy C, et al. Postconditioning with a volatile anaesthetic in alveolar epithelial cells in vitro. *Eur Respir J.* 2008; 31(1):118–25. <https://doi.org/10.1183/09031936.00046307> PMID: 17898018.
21. Rist RJ, Romero IA, Chan MW, Couraud PO, Roux F, Abbott NJ. F-actin cytoskeleton and sucrose permeability of immortalised rat brain microvascular endothelial cell monolayers: effects of cyclic AMP and astrocytic factors. *Brain Res.* 1997; 768(1–2):10–8. PMID: 9369295.
22. Yeh WL, Lin CJ, Fu WM. Enhancement of glucose transporter expression of brain endothelial cells by vascular endothelial growth factor derived from glioma exposed to hypoxia. *Mol Pharmacol.* 2008; 73(1):170–7. <https://doi.org/10.1124/mol.107.038851> PMID: 17942749.
23. Davis B, Tang J, Zhang L, Mu D, Jiang X, Biran V, et al. Role of vasodilator stimulated phosphoprotein in VEGF induced blood-brain barrier permeability in endothelial cell monolayers. *Int J Dev Neurosci.* 2010; 28(6):423–8. <https://doi.org/10.1016/j.ijdevneu.2010.06.010> PMID: 20599605; PubMed Central PMCID: PMC3519884.
24. Carpenter AE, Jones TR, Lamprecht MR, Clarke C, Kang IH, Friman O, et al. CellProfiler: image analysis software for identifying and quantifying cell phenotypes. *Genome Biol.* 2006; 7(10):R100. <https://doi.org/10.1186/gb-2006-7-10-r100> PMID: 17076895; PubMed Central PMCID: PMC3519459.
25. Prakash R, Carmichael ST. Blood-brain barrier breakdown and neovascularization processes after stroke and traumatic brain injury. *Curr Opin Neurol.* 2015; 28(6):556–64. <https://doi.org/10.1097/WCO.000000000000248> PMID: 26402408.
26. Al Ahmad A, Gassmann M, Ogunshola OO. Maintaining blood-brain barrier integrity: pericytes perform better than astrocytes during prolonged oxygen deprivation. *J Cell Physiol.* 2009; 218(3):612–22. <https://doi.org/10.1002/jcp.21638> PMID: 19016245.
27. Mark KS, Davis TP. Cerebral microvascular changes in permeability and tight junctions induced by hypoxia-reoxygenation. *Am J Physiol Heart Circ Physiol.* 2002; 282(4):H1485–94. <https://doi.org/10.1152/ajpheart.00645.2001> PMID: 11893586; PubMed Central PMCID: PMC3519411.
28. Komarova Y, Malik AB. Regulation of endothelial permeability via paracellular and transcellular transport pathways. *Annu Rev Physiol.* 2010; 72:463–93. <https://doi.org/10.1146/annurev-physiol-021909-135833> PMID: 20148685.
29. Tornavaca O, Chia M, Dufton N, Almagro LO, Conway DE, Randi AM, et al. ZO-1 controls endothelial adherens junctions, cell-cell tension, angiogenesis, and barrier formation. *J Cell Biol.* 2015; 208(6):821–38. <https://doi.org/10.1083/jcb.201404140> PMID: 25753039; PubMed Central PMCID: PMC3519456.
30. Cattelino A, Liebner S, Gallini R, Zanetti A, Balconi G, Corsi A, et al. The conditional inactivation of the β -catenin gene in endothelial cells causes a defective vascular pattern and increased vascular fragility. *The Journal of Cell Biology.* 2003; 162(6):1111–22. <https://doi.org/10.1083/jcb.200212157> PMID: 12975353

31. Liang D, Bhatta S, Gerzanich V, Simard JM. Cytotoxic edema: mechanisms of pathological cell swelling. *Neurosurg Focus*. 2007; 22(5):E2. PMID: [17613233](#); PubMed Central PMCID: PMCPMC2740913.
32. Tzur A, Moore JK, Jorgensen P, Shapiro HM, Kirschner MW. Optimizing optical flow cytometry for cell volume-based sorting and analysis. *PLoS One*. 2011; 6(1):e16053. <https://doi.org/10.1371/journal.pone.0016053> PMID: [21283800](#); PubMed Central PMCID: PMCPMC3024321.
33. Basiji DA, Ortyn WE, Liang L, Venkatachalam V, Morrissey P. Cellular image analysis and imaging by flow cytometry. *Clin Lab Med*. 2007; 27(3):653–70, viii. <https://doi.org/10.1016/j.cll.2007.05.008> PMID: [17658411](#); PubMed Central PMCID: PMCPMC2034394.
34. Ilan N, Tucker A, Madri JA. Vascular endothelial growth factor expression, beta-catenin tyrosine phosphorylation, and endothelial proliferative behavior: a pathway for transformation? *Lab Invest*. 2003; 83(8):1105–15. PMID: [12920240](#).
35. Wang W, Dentler WL, Borchardt RT. VEGF increases BMEC monolayer permeability by affecting occludin expression and tight junction assembly. *Am J Physiol Heart Circ Physiol*. 2001; 280(1):H434–40. PMID: [11123261](#).
36. Sims D, Duchek P, Baum B. PDGF/VEGF signaling controls cell size in *Drosophila*. *Genome Biol*. 2009; 10(2):R20. <https://doi.org/10.1186/gb-2009-10-2-r20> PMID: [19216764](#); PubMed Central PMCID: PMCPMC2688285.
37. van Bruggen N, Thibodeaux H, Palmer JT, Lee WP, Fu L, Cairns B, et al. VEGF antagonism reduces edema formation and tissue damage after ischemia/reperfusion injury in the mouse brain. *J Clin Invest*. 1999; 104(11):1613–20. <https://doi.org/10.1172/JCI8218> PMID: [10587525](#); PubMed Central PMCID: PMCPMC409867.
38. Kimura R, Nakase H, Tamaki R, Sakaki T. Vascular endothelial growth factor antagonist reduces brain edema formation and venous infarction. *Stroke*. 2005; 36(6):1259–63. <https://doi.org/10.1161/01.STR.0000165925.20413.14> PMID: [15879344](#).
39. Doherty GJ, McMahon HT. Mediation, modulation, and consequences of membrane-cytoskeleton interactions. *Annu Rev Biophys*. 2008; 37:65–95. <https://doi.org/10.1146/annurev.biophys.37.032807.125912> PMID: [18573073](#).
40. Hayes S. Adherens junctions: which way is up? *Nat Cell Biol*. 2006; 8(10):1052. <https://doi.org/10.1038/ncb1006-1052> PMID: [17013418](#).
41. Pan C, Kumar C, Bohl S, Klingmueller U, Mann M. Comparative proteomic phenotyping of cell lines and primary cells to assess preservation of cell type-specific functions. *Mol Cell Proteomics*. 2009; 8(3):443–50. <https://doi.org/10.1074/mcp.M800258-MCP200> PMID: [18952599](#); PubMed Central PMCID: PMCPMC2649808.